

DSC study on Mg-Si phases in as cast AA6xxx

N.C.W. Kuijpers¹, W.H. Kool², S. van der Zwaag^{1,2}

¹*Netherlands Institute of Metals Research (NIMR), Rotterdamseweg 137, 2628 AL Delft, The Netherlands.*

²*Laboratory for Materials Science, Delft University of Technology, Rotterdamseweg 137, 2628 AL Delft, The Netherlands.*

Keywords: DSC, precipitation, precipitates, intermetallics, Mg₂Si

Abstract. As cast billets of AA6xxx alloys require a homogenisation treatment to make the material suitable for hot extrusion. During this homogenisation treatment several processes take place such as the transformation of interconnected plate-like β -Al₅FeSi intermetallics into more rounded discrete α -Al₁₂(FeMn)₃Si particles and the dissolution of β -Mg₂Si particles. Precipitation and dissolution of Mg-Si phases in as cast material were investigated for various Fe contents (0.02 wt%, 0.19 wt% and 0.65 wt%) by means of DSC measurements and optical microscopy. Eutectic melting was also studied. In as cast material, the amount of Fe-containing intermetallics increases with Fe content. It appears that the amount of precipitation of β'' and β' Mg-Si phases during the DSC scan is lower for higher Fe content and that the corresponding activation energies are similar and independent of the Fe content. The amount of eutectic melting is dependent on the time involved with the DSC scan.

Introduction

As cast billets of AA6xxx require a homogenisation treatment to make the material suitable for hot extrusion. During this homogenisation treatment several processes take place such as the transformation of interconnected plate-like β -Al₅FeSi intermetallics into more rounded discrete α_c -Al₁₂(FeMn)₃Si particles and the dissolution of β -Mg₂Si particles [1]. Transformation of β -Al₅FeSi to α_c -Al₁₂(FeMn)₃Si intermetallics is important because it improves the ductility of the material [2]. Dissolution of β -Mg₂Si is also important since it will give maximum age hardening potential for the extruded product and will suppress the generation of surface defects due to local melting [3,4]. Although the precipitation and dissolution of Mg-Si phases in already homogenised and aged material have been studied in detail [5-7], such studies are not found for as cast materials.

It is known that the concentration of Fe influences the β -Al₅FeSi to α_c -Al₁₂(FeMn)₃Si transformation kinetics and the amount and morphology of these phases [8]. Also some influence of Fe on the precipitation and dissolution of the Mg-Si phases might be expected. A strong influence of the Fe content on the diffusion of Mg and Si or their solubility is not anticipated since for a very low Fe content the maximum solubility of Fe in Al has already been reached. Therefore, the activation energies of dissolution and precipitation of Mg-Si phases are expected to be independent of Fe content.

However, an indirect influence of the Fe content might be present since Fe will affect the morphology and spatial distribution of the Fe containing intermetallics in the eutectic and therefore that of the Mg₂Si particles in the eutectic. Furthermore, the Si concentration in the matrix may depend on the Fe content because of the incorporation of Si in the Fe containing intermetallics.

The aim of this study is to investigate precipitation, dissolution and eutectic melting of Mg-Si particles in the as cast structure of AA6xxx for various Fe contents. To this purpose both optical microscopy and Differential Scanning Calorimetry (DSC) measurements were performed.

Experimental

Materials and microstructural characterisation. Table 1 shows the compositions of three as cast Al-Mg-Si-Fe alloys. The Mg and Si contents in each alloy are approximately equal whereas the Fe content varies between 0.02 and 0.65 wt%. Since these alloys do not contain Mn, the Fe containing intermetallics consist of β -Al₅FeSi and/or α_c -Al₁₂Fe₃Si. The alloys were cast in steel moulds of 200 mm x 150 mm x 400 mm and subsequently air cooled. All samples for optical characterisation and DSC measurements were taken at least 20 mm from the edge of the ingot to get a similar microstructure and composition.

Table 1. Alloy composition [wt%] for alloys A, B and C.

Alloy	Mg	Si	Fe	Other	Al
A	0.75	0.52	0.02	<0.01	Balanced
B	0.76	0.45	0.19	<0.01	Balanced
C	0.82	0.49	0.65	<0.01	Balanced

In the optical micrographs, the Al matrix appears as light grey areas, the β -Al₅FeSi and α_c -Al₁₂Fe₃Si intermetallics as medium grey particles and the β -Mg₂Si as dark grey particles. Also differences in morphology between the different types of particles are visible. The volume fraction of the intermetallics in each casting was determined. By automatic SEM and EDX measurements the volume fraction of α_c -Al₁₂Fe₃Si and β -Al₅FeSi was determined, which method is described in detail in Ref. [9].

DSC measurements. DSC measurements were performed using a Perkin and Elmer DSC7 with a sample weight of approximately 60 mg. Pure aluminium was used as a reference. Temperature scans were made from 20°C to 605°C with constant heating rates of 5, 10, 20 or 40 °C/min. A baseline was obtained by fitting a polynomial at points in the curve where no reactions occurred. The activation energies of the precipitation of β'' and β' Mg-Si and the precipitation and dissolution of β -Mg₂Si were obtained by the Kissinger method [4,10,11]. The activation energy Q is determined from the slope of the straight line obtained by plotting $\ln(T_p^2/\dot{f})$ versus $1/RT_p$, where T_p is the peak temperature of the reaction, \dot{f} is the heating rate and R is the gas constant.

Results

Optical microscopy. Fig. 1 shows micrographs of two as cast microstructures (alloys B and C). The intermetallics and the Mg-Si particles are clearly distinguishable. The particles are plate-like and appear as needles in the micrographs [12]. The Mg-Si particles are precipitated as β -Mg₂Si on the boundaries of the Fe containing particles, as isolated β -Mg₂Si particles on the boundaries of the Al-dendrites, or as much smaller β -Mg₂Si or β' Mg-Si precipitates in the matrix. The larger β -Mg₂Si particles, present in the interdendritic liquid accompanying the eutectic reaction during casting, are more spherical with a diameter of approximately 2 μ m or larger. The β -Mg₂Si or β' Mg-Si particles in the Al matrix have a needle shape and their width is smaller than 0.5 μ m. They are precipitated from the supersaturated solid matrix during cooling of the casting. Close to the Fe containing particles there is a solute depleted zone where no Mg-Si particles are precipitated.

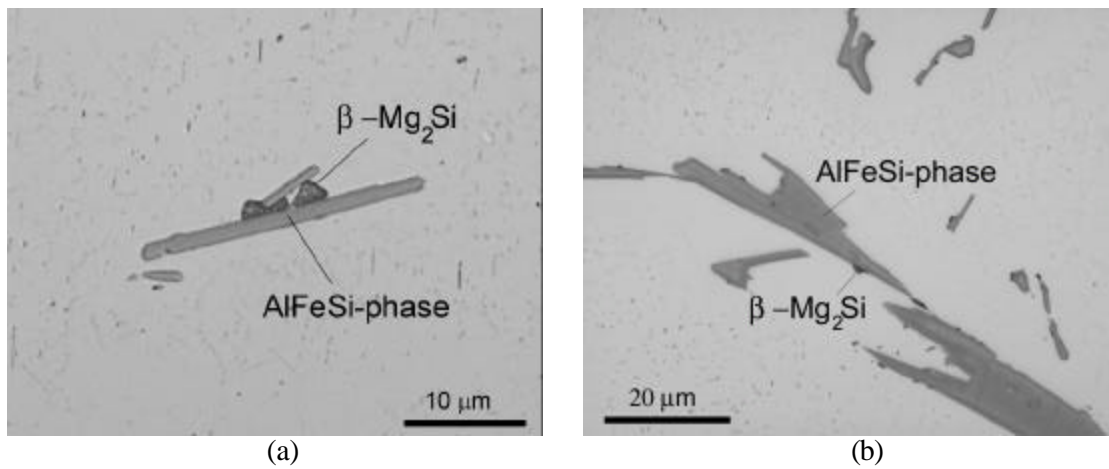


Fig. 1 Optical micrographs of alloys B (a) and C (b).

Table 2 gives an overview of the measured volume concentration of β - Al_5FeSi and α_c - $\text{Al}_{12}\text{Fe}_3\text{Si}$ intermetallics. Also the calculated volume concentration of intermetallics is given assuming that all Fe in the alloy is bound in the intermetallic phases. The volume fraction of intermetallics increases as the Fe content increases. The calculated intermetallic volume fraction is slightly higher than the measured fraction, since some Fe is in solid solution or precipitated in small particles which were not detected by the imaging system. Measurement of the amount of Mg-Si and β - Mg_2Si particles present in the matrix was not possible because most particles were too small to analyse quantitatively by optical or SEM measurement.

Table 2. Volume concentrations [vol.%] of intermetallic phases present.

Alloy	α_c - $\text{Al}_{12}\text{Fe}_3\text{Si}$ (measured)	β - Al_5FeSi (measured)	α_c - $\text{Al}_{12}\text{Fe}_3\text{Si}$ + β - Al_5FeSi (calculated)
A	<0.1	<0.1	<0.1
B	0.3 ± 0.1	0.1 ± 0.1	0.5
C	0.6 ± 0.2	0.6 ± 0.2	1.9

DSC measurements. DSC scans of alloys A, B and C are shown in Fig. 2 for a heating rate of $40^\circ\text{C}/\text{min}$. Six peaks are visible in the plots, indicated by (1) to (6). The exothermic peak (1), with a maximum at approximately 320°C , is due to the formation of β'' Mg-Si particles [5]. The exothermic peak (2), with a maximum at approximately 350°C , is caused by the formation of β' Mg-Si particles [5]. There is a large overlap of the peaks (1) and (2). The exothermic peak (3), with a maximum at approximately 450°C , is caused by the precipitation of β - Mg_2Si particles [5]. The endothermic peak (4), with maximum at approximately 540°C , is due to the dissolution of the Mg_2Si particles. The small endothermic peak (5), with an onset of approximately 578°C , is caused by eutectic melting of $\text{Al} + \text{Mg}_2\text{Si} + \beta$ - $\text{Al}_5\text{FeSi} \rightarrow \text{L} + \alpha'$ - $\text{Al}_8\text{Fe}_2\text{Si}$ [3]. It appears only in the alloy with a high Fe content (alloy C). The endothermic peak (6), with an onset temperature of approximately 587°C , is caused by the eutectic melting of $\text{Al} + \text{Mg}_2\text{Si} \rightarrow \text{L}$ [13].

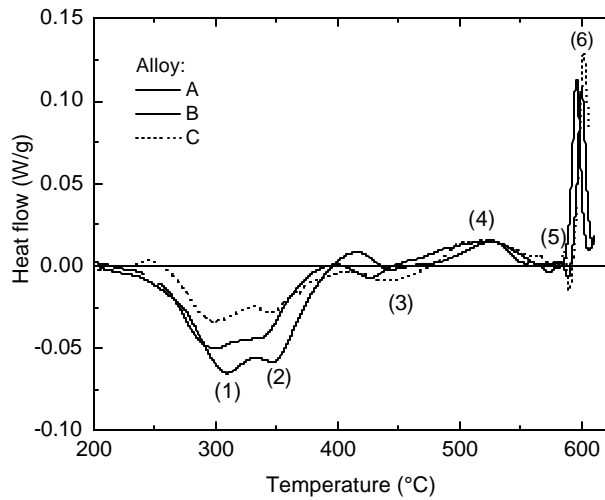


Fig. 2 DSC scans for alloys A, B and C; heating rate: 40°C/min. The characteristic peaks are indicated by (1) to (6).

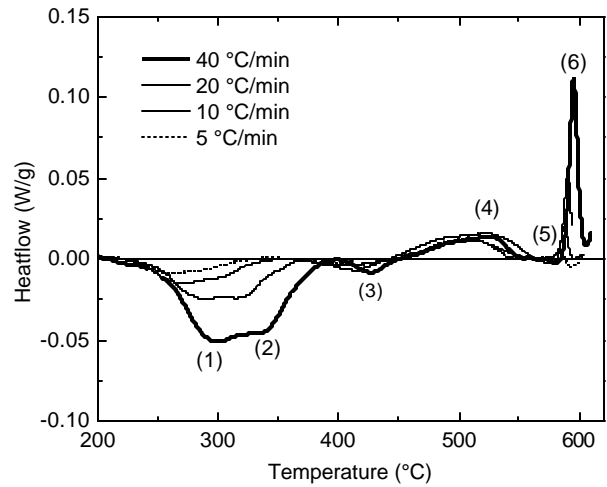


Fig. 3 DSC scans for alloy B for various heating rates.

It is found that peaks (1) and (2) decrease as a function of Fe content, which means that fewer β'' and β' Mg-Si particles are precipitated. Since more Si is bound to the Fe containing particles in alloys with higher Fe content, the resulting Si concentration in solute solution is lower and precipitation of β'' and β' Mg-Si particles will decrease. As the intensity and position of peak (4) are independent of Fe content, the dissolution of the Mg_2Si particles is not influenced by the Fe content.

Kinetics of precipitation and dissolution of Mg-Si phases. Fig. 3 presents the DSC results of alloy B for various heating rates. The peak temperatures of peak (1) to (4) shift as a function of heating rate. Fig. 4 shows the Kissinger plots of peak (1) to (3) of alloy B. Straight lines are observed for this alloy and also for alloys A and C. Table 3 summarises the activation energies obtained from the Kissinger plots. Within experimental error, the activation energies of β'' and β' precipitation are the same for all three alloys. The activation energies for the precipitation of β - Mg_2Si are higher but also the same for the three alloys.

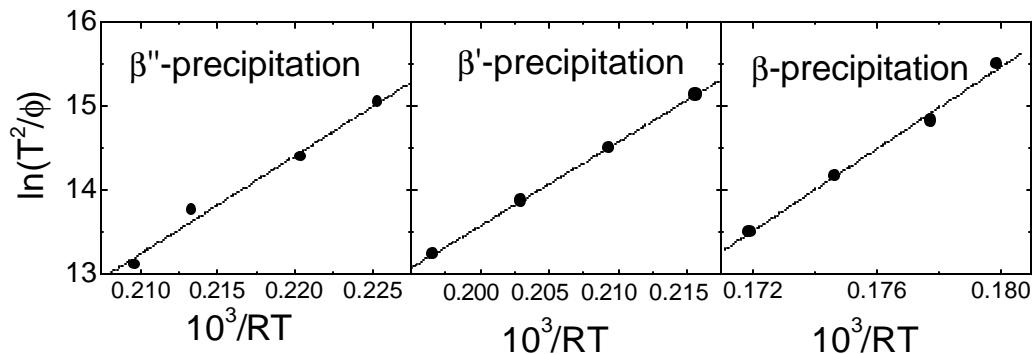


Fig. 4 Kissinger plots of the different peaks found for alloy B.

The activation energies measured correspond well with those derived from the data published by Doan *et al.* [5], which results are also given in Table 3. The activation energies of the precipitation of β'' and β' are close to the reported activation energies for diffusion of Mg and Si in Al, which are in the range of 120-140 kJ/mol [14,15].

The activation energies, determined from the Kissinger plots for peak (4) (dissolution of β - Mg_2Si) are in the range of 500 ± 250 kJ/mol and are much higher than the activation energies reported above, in spite of the large uncertainty in the values. Also from the published data in Ref. [3], we derive comparable high values.

In Fig. 5 the released heat of β - Mg_2Si dissolution (peak 4) is plotted as a function of heating rate. The heat of dissolution decreases with increasing heating rate, which implies that at a higher heating rate less β - Mg_2Si gets dissolved. Within experimental error no effect of Fe content was found.

Table 3. Activation energies found by the Kissinger method. Values derived from literature data for AA6061 [5] are also given.

Alloy	β'' precipitation [kJ/mol]	β' precipitation [kJ/mol]	β - Mg_2Si precipitation [kJ/mol]
A	115 ± 10	110 ± 10	175 ± 15
B	117 ± 10	100 ± 10	182 ± 15
C	125 ± 10	112 ± 10	170 ± 15
AA6061	105	93	100-300

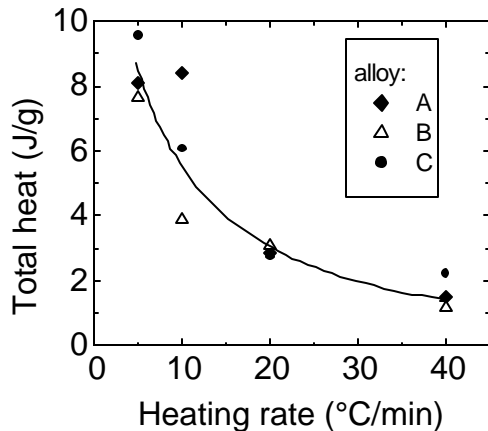


Fig. 5 The released heat of β - Mg_2Si dissolution for alloys A, B and C.

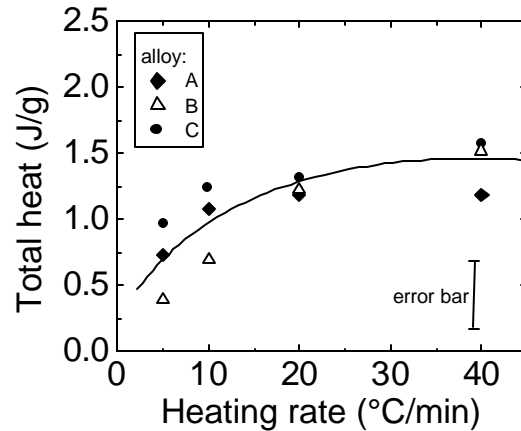


Fig. 6 The released heat of eutectic melting for alloys A, B and C.

Eutectic melting. In Fig. 6 the heat released with eutectic melting (peak (6)) is plotted as a function of heating rate. It is found that the total heat increases as a function of heating rate which means that less β - Mg_2Si is present in the microstructure after heating till the onset of peak (6). This trend corresponds with the trend as presented in Fig. 5, indicating that during the DSC scan for high heating rates less β - Mg_2Si gets dissolved, and that more β - Mg_2Si remains in the eutectic and contributes to eutectic melting. Within experimental error no effect of Fe content was found.

Conclusion

- 1) The amount of β'' and β' Mg-Si precipitation is lower for higher Fe content. This is attributed to the incorporation of a part of the Si into the α_c - $Al_{12}Fe_3Si$ and β - Al_5FeSi intermetallics and consequently to a lower Si solute level.

- 2) Activation energies for the β'' and β' Mg-Si precipitation are similar and correspond well to the literature data. They are independent of the Fe content in the alloy. The activation energies of the β -Mg₂Si precipitation are higher than those obtained for β'' and β' Mg-Si precipitation and are also independent of the alloy content in the alloy. The activation energy of β -Mg₂Si dissolution is much higher.
- 3) The heat connected with the eutectic melting of Al + β -Mg₂Si decreases for lower heating rates. During the DSC-scan a certain amount of homogenisation of the as cast alloy has already taken place, leading to a lower amount of eutectic left at the onset of eutectic melting.

Acknowledgements

This research was carried out under project number MP 97009-3 in the framework of the strategic research program of the Netherlands Institute for Metals Research in the Netherlands (www.nimr.nl). The authors acknowledge Peter Koenis of BOAL, de Lier, for the SEM characterisation of the materials.

References

- [1] S. Zajac, B. Hutchinson, A. Johansson, L.O. Gullman, *Mat. Sci. and Tech.* **10** (1994) 323.
- [2] J. Langerweger, *Proc. of Conf. on Aluminium Technology*, London, March 1986 (1986) 216.
- [3] T. Minoda, H. Hayakawa, H. Yodida, *Sumitomo Light Metal Technical Reports* **39** No. 1 (1998) 26.
- [4] K. Karhausen, A.L. Dons, T. Aukrust, *Mat. Sci. Forum* **217-222** (1996) 403.
- [5] L.C. Doan, Y. Ohmori and K. Nakai, *Mat. Trans. JIM* **41** No 2 (2000) 300.
- [6] S.P. Chen, M.S. Vossenbergh, F.J. Vermolen, J. van de Langkruis, *Mat. Sci. and Eng. A* **A272** (1999) 199.
- [7] H. Westengen, N. Ryum, *Z. Metallkunde* **70** (1979) 528.
- [8] H. Tanihata, T. Sugawara, K. Matsuda, S. Ikeno, *J. Mat. Sci.* **34** (1999) 1205.
- [9] N.C.W. Kuijpers, W.H. Kool, P. Koenis, K. Nilsen, S. v.d. Zwaag, "Assessment of quantification of \mathbf{b} -AlFeSi and \mathbf{a}_c -Al(FeMn)Si in 6xxx Al series", to be submitted.
- [10] H.E. Kissinger, *Anal. Chem.* **29** (1957) 1702.
- [11] S.P. Chen, K.M. Mussert, S. van der Zwaag, *J. Mat. Sci.* **33** (1998) 4477.
- [12] J. Tirel, D. Hanlon, N.C.W. Kuijpers, S. van der Zwaag, "Quantification of the evolution of the 3D intermetallic structure in a 6005A aluminium alloy during a homogenisation treatment.", to be submitted.
- [13] N. Chakraborti, H.L. Lukas, *Calphas* **16** (1992) 79.
- [14] S. Fujikawa, K. Hirano, Y. Fukushima, *Mat. Trans. A.* **9A** (1978) 1811.
- [15] S.I. Fujikawa, *Defects and Diffusion Forum* **143-147** (1997) 403.